Catalysis Today 158 (2010) 510–514

Contents lists available at ScienceDirect

Catalysis Today

journal homepage: www.elsevier.com/locate/cattod

Ethanol-assistant synthesis of TS-1 containing no extra-framework Ti species

Deng-Gao Huang, Xian Zhang, Bao-Hui Chen, Zi-Sheng Chao*

College of Chemistry and Chemical Engineering, Key Laboratory of Chemometrics & Chemical Biological Sensing Technologies, Ministry of Education, Hunan University, Changsha, Hunan 410082, China

ARTICLE INFO

Article history:
Available online 17 September 2010

Keywords:
TS-1
Synthesis
Ethanol
Cyclohexanone
Ammoximation

ABSTRACT

Titanium silicate-1 (TS-1) was synthesized via three different procedures, respectively, using tetraethylorthosilicate (TEOS) and tetrabutyl orthotitanate (TBOT) as Si and Ti sources and tetrapropylammonium hydroxide (TPAOH) as template. In the procedures *A* and *B*, ethanol and isopropanol were respectively employed as the solvents of TBOT and were remained all through the hydrothermal crystallization of TS-1. In the procedure *C*, isopropanol was also employed as the solvent of TBOT but was evaporated before the crystallization step. The TS-1 specimens synthesized via the three procedures were characterized by means of XRD, FT-IR, DRS UV–vis, SEM, N_2-physisorption and NH_3-TPD. It was shown that, the contents of framework Ti species in the TS-1 basing on the procedures *A* and *C* were comparable, being both larger than that basing on the procedure *B*. Extra-framework Ti, anatase, was absent in the TS-1 basing on the procedure *A* but present in the TS-1 basing on the procedures *B* and *C*, with its content being larger for the procedure *B* than for the procedure *C*. The extra-framework Ti might disperse highly both on the surfaces and in the micropores of TS-1. The framework Ti contributed the weak acid sites and the extra-framework Ti the strong acid sites of TS-1. The catalytic performance for the ammoximation of cyclohexanone over the TS-1 synthesized via various procedures was evaluated and the yield of cyclohexanone–oxime was found to follow an order procedure *A* > procedure *C* > procedure *B*. It was concluded that the TS-1 with a large content of framework Ti but without anatase, exhibiting high catalytic performance, could be effectively synthesized by the employment of ethanol.

1. Introduction

Titanium silicate-1 (TS-1) is a titanosilicate zeolite with a MFI structure. The main feature of this zeolite is the presence of Ti atoms as atomically dispersed species, which substitutes isomorphously a small fraction of Si atoms in the tetrahedral sites of silicalite-1 framework. This endows TS-1 with a few unique properties, such as, the large coordination ability of Ti^{4+} ions, the high hydrophobicity and the excellent shape selectivity. Since its first report by Taramasso et al. in 1983 [1], TS-1 has been paid much attention and found large potential applications in a series of clean oxidative reactions under mild conditions and using hydrogen peroxide as oxidant, for examples, the selective oxidations of olefins to epoxies, alcohols to aldehydes or ketones, the hydroxylations of aromatics, and the ammoximation of cyclohexanone [2–5].

TS-1 is usually hydrothermally synthesized, employing silicon and titanium ethoxides, as the Si and Ti sources, and organic base, typically tetrapropylammonium hydroxide (TPAOH), as the structure directing agent and mineralizer [1]. During the synthesis of TS-1, the hydrolysis/condensation of Si and Ti sources, and particularly the hydrolysis of Ti sources to form a Ti-gel, constitutes the key step, which has been found to affect largely the content and existing state of Ti in the final TS-1 [6]. It is known that, the more framework Ti the TS-1 contains, with a maximum value of 2.5 wt% [7], the higher catalytic performance the TS-1 would present. The presence of anatase reduces significantly the catalytic performance of TS-1, because of its promotion to the decomposition of H_2O_2 [8,9]. In the original report by Taramasso et al. [1], TS-1 was synthesized from the Si–Ti co-gel, which was prepared via the first addition of the Ti source, tetraethylorthotitanate (TEOT), into the Si source, tetraethylorthosilicate (TEOS), followed by the gradual addition of the aqueous solution of the TPAOH template. But the TS-1 obtained by this method contained only very small amount of framework Ti, because the hydrolysis speed of TEOT was far faster than that of TEOS. Whereas many attempts have been made to increase the content of framework Ti, it is still a challenge that the increase of the isolated tetrahedral Ti in the TS-1 framework is usually accompanied by the formation of extra-framework Ti, usually anatase, due to the strong tendency of the polymerization of Ti under aqueous conditions [6]. In 1990s, it was found that a hydrophobic environment favored the formation of framework Ti, and the mixing of anhydrous isopropanol (IPA) with titanium ethoxides before the

* Corresponding author. Tel.: +86 731 88713257; fax: +86 731 88713257.
E-mail addresses: zschao@yahoo.com, chao_zs@yahoo.com.cn (Z.-S. Chao).

0920-5861/$ – see front matter © 2010 Elsevier B.V. All rights reserved.
doi:10.1016/j.cattod.2010.07.027

hydrolysis of titanium ethoxides was proven to be an effective route to prevent from the precipitation of TiO_2 [10–12]. However, isopropanol (IPA) had to be distillated out after the formation of the Ti–Si gel in the subsequent step, since IPA in the solution tended to hold the Ti species out of the TS-1 framework. This introduced the additional complexity and cost for the synthesis of TS-1.

In the present paper, we showed a novel synthesis of TS-1, involving the replacement of IPA by ethanol at no requirement for the distillation of ethanol from the batch. Compared to that synthesized via the conventional procedure, which involved the employment of IPA before the hydrolysis of tetrabutyl orthotitanate (TBOT) and its removal after the hydrolysis of TBOT, the TS-1 synthesized by our novel method possessed an appreciably high content of framework Ti species without the presence of extra-framework Ti and exhibited much more higher catalytic performance for the ammoximation of cyclohexanone.

2. Experimental

2.1. Chemicals

The chemicals involved in the synthesis of TS-1 and the catalytic reaction were as follows: TEOS (99%), TBOT (98%), TPAOH (1.5 M solution in water), ethanol (99.7%), IPA (99.5%), t-butanol (99%), cyclohexanone (98.5%), hydrogen peroxide (H_2O_2, 30%) and ammonia (NH_3, 99.9%).

2.2. Synthesis of TS-1 via various procedures

Procedure A. 98.1 ml TEOS, 70.5 ml TPAOH and 113 ml H_2O were first added into a 500 ml three-neck flask, at room temperature and under strong stirring, allowing the hydrolysis of TEOS for 1 h. Then, a solution of 4.88 ml TBOT in 50 ml ethanol was added dropwise at ice-bath temperature and under strong stirring. After the addition, the mixture was stirred for another 1 h, and then, the temperature was raised to 333 K, allowing the hydrolysis of TBOT for 1 h, resulting in a sol with a molar composition SiO_2:0.033 TiO_2:0.20 TPAOH:2.0 Ethanol:20 H_2O. This sol was transferred into a Teflon-lined autoclave and subjected to a hydrothermal crystallization at 443 K for 4 d. After crystallization, the solid was recovered by centrifugal separation, washing repeatedly with deionized water, drying at 393 K for 12 h and then calcination at 823 K for 12 h. The as-synthesized specimen was denoted as *A*.

Procedure B. A sol with a molar composition SiO_2:0.033 TiO_2:0.20 TPAOH:1.5 IPA:20 H_2O was first prepared as above for *A*, except that 50 ml ethanol was replaced with 50 ml IPA in the batch. Then, the sol was subjected to the same treating procedure as above for *A*, and the specimen resulted was denoted as *B*.

Procedure C. A sol with the same composition as above for *B* was first prepared and then heated at 354 K to evaporate the alkanol (ethanol and IPA). The resultant mixture was subjected to the same treating procedure as above for *A*, and the specimen obtained was denoted as *C*.

2.3. Characterization of TS-1

X-ray diffraction spectroscopy (XRD) was performed with a Bruker D8 Advance X-ray diffractometer, under the conditions of Cu target (K_α ray, λ = 1.54187 Å), scanning voltage 40 kV, scanning current 40 mA, scanning speed 0.2 s and scanning step 0.02°.

Diffuse reflectance (DR UV–vis) spectroscopy was carried out using a Perkin Elmer Lambda 35 spectrometer, equipped with deuterium and tungsten lamps, using $BaSO_4$ as standard.

Fourier transform infrared (FT-IR) spectroscopy was recorded on a Varian 3100 spectrometer with a DTGS detector and a CeI beamsplitter. The data were recorded from 400 to 2000 cm^{-1} at a scanning number of 40 and a resolution of 4 cm^{-1}.

Scanning electron microscopy (SEM) was conducted by a JSM-6700 scanning electron microscope with an accelerating voltage of 5 kV.

NH_3 temperature programmed desorption (NH_3-TPD) was determined on a Micromeritics AutoChem II 2920 instrument equipped with a thermal conductivity detector (TCD). The TS-1 specimen was first degassed in a flow of helium with a flow rate of 50 ml/min at 773 K for 30 min, followed by cooling to 373 K. Then, NH_3 was repeatedly pulse-injected until its saturation adsorption over the specimen had been achieved. After that, NH_3 was desorbed by heating the specimen from 373 to 1023 K at a rate of 15 K/min. During the adsorption and desorption of NH_3, the helium flow was retained and its flow rate was maintained constant at 60 ml/min.

N_2-physisorption was performed at liquid nitrogen temperature using a Quantachrome Autosorb-1 instrument. Before the adsorption measurement, the specimen was degassed for 16 h at a temperature of 573 K under a residual pressure lower than 4×10^{-4} Pa in the degas port of the adsorption apparatus. The specific surface area was calculated by using the multipoint BET equation. The pore size and its distribution were obtained from the N_2-desorption branch by applying the SF method. The pore volume and area were calculated by using the *t*-plot micropore analysis method.

2.4. Oximation of cyclohexanone with TS-1 catalyst

The oximation of cyclohexanone was performed in a round-bottomed flask, equipped with a condenser and a magnetic stirrer, at 353 K and under the atmospheric pressure. The TS-1 prepared above were employed as the catalysts, a 30% H_2O_2 aqueous solution and NH_3 gas as the oxidant and an equal molar mixture of water and t-butanol as solvent. The reaction batch had a weight ratio solvent:catalyst:cyclohexanone = 60:1:10 and a molar ratio cyclohexanone:NH_3:H_2O_2 = 1:1.5:1.2. After 2 h of reaction, the products mixture was analyzed by a Varian 3800 gas chromatography equipped with a flame ionization detector (FID) and a SE-54 capillary column (0.25 mm × 50 m).

3. Results and discussion

Fig. 1 presents the XRD patterns of the specimens *A*–*C*. One can see that all of the specimens exhibit a set of diffraction peaks at 2θ = 7.9°, 8.8°, 23.1°, 23.9° and 24.4° in their XRD patterns, indicating the presence of TS-1 [13,14]. The peak intensities of TS-1 for the specimens *A*–*C* are almost same, showing a comparable level of

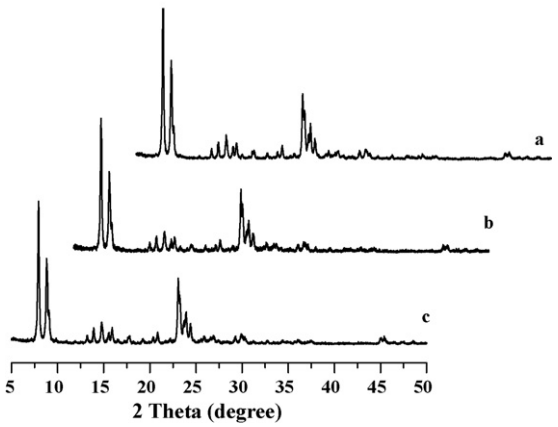

Fig. 1. XRD patterns of the specimens (a) *A*, (b) *B* and (c) *C*.

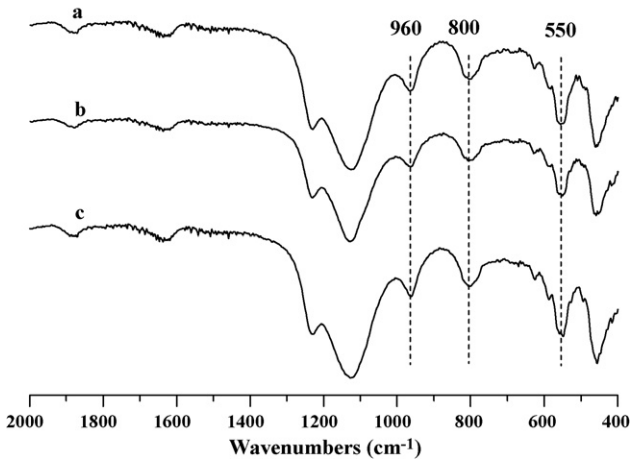

Fig. 2. FT-IR spectra of the specimens (a) *A*, (b) *B* and (c) *C*.

TS-1 crystallinity. Except TS-1, no amorphous phase and separated anatase can be identified in Fig. 1.

Fig. 2 illustrates the FT-IR spectra of the specimens *A*–*C*. The absorption band at 550 cm^{-1} is an indicative of MFI structure [15]. The absorption band at 960 cm^{-1}, being attributed to the stretching mode of [SiO_4] units bonded to a Ti^{4+} ion (O_3SiOTi), indicates the incorporation of titanium in the MFI framework [16]. For TS-1, the level of titanium incorporated into the framework is usually estimated by the band intensity ratio I_{960}/I_{800} [17] or I_{960}/I_{550} [18]. The higher the ratio, the larger is the content of framework Ti. Both of the ratios for the specimens *A*–*C* are calculated and the results are listed in Table 1, which shows that the content of framework Ti has an order specimens *A* ≈ specimens *C* > specimens *B*.

Fig. 3 shows the SEM micrographs of the specimens *A*–*C*. One can see that all of the specimens have the morphology of regular polyhedron with a very narrow pore size distribution. The average size of the specimens *A*–*C* is determined as ca. 168, 152 and 120 nm, respectively. No amorphous phase can be observed from the micrographs.

Fig. 4 shows the DR UV–vis spectra of the specimens *A*–*C*. All of the specimens display a broad absorption band centered at ca. 250 nm. In addition, the specimens *B* and *C* exhibit a shoulder at ca. 320 and 340 nm, respectively. The absorption at 320–340 nm is ascribed to extra-framework Ti, usually in the form of anatase [19]. The broad absorption band at ca. 250 nm can be assigned to a low-energy charge-transfer transition between tetrahedral oxygen ligands and framework Ti^{4+} ions [16,20]. It is also possible that the broad band at 250 nm is a result of the combination of the bands at 210–230 and 270–280 nm, both of which are often reported for TS-1 in the literature [21]. The band at 210–230 nm originates from the charge transfer between the 2p electron of tetrahedral oxygen ligand and the empty 3d orbital of framework Ti^{4+} ion [22]. The band at 270–280 nm was assigned in some literatures to isolated hexa-coordinated Ti species containing two water molecules in the coordination sphere [16,22]. We have found, however, that there is no difference between the DR UV–vis spectra for the specimens *A*–*C* prepared freshly and for those exposed to water in air. Thus,

Table 1
Ratios I_{960}/I_{800} and I_{960}/I_{550} for the 960, 880 and 550 cm^{-1} absorption bands in the FT-IR spectra of specimens *A*–*C*.

Ratio	Specimens		
	A	*B*	*C*
I_{960}/I_{800}	0.563	0.43	0.568
I_{960}/I_{550}	0.489	0.438	0.487

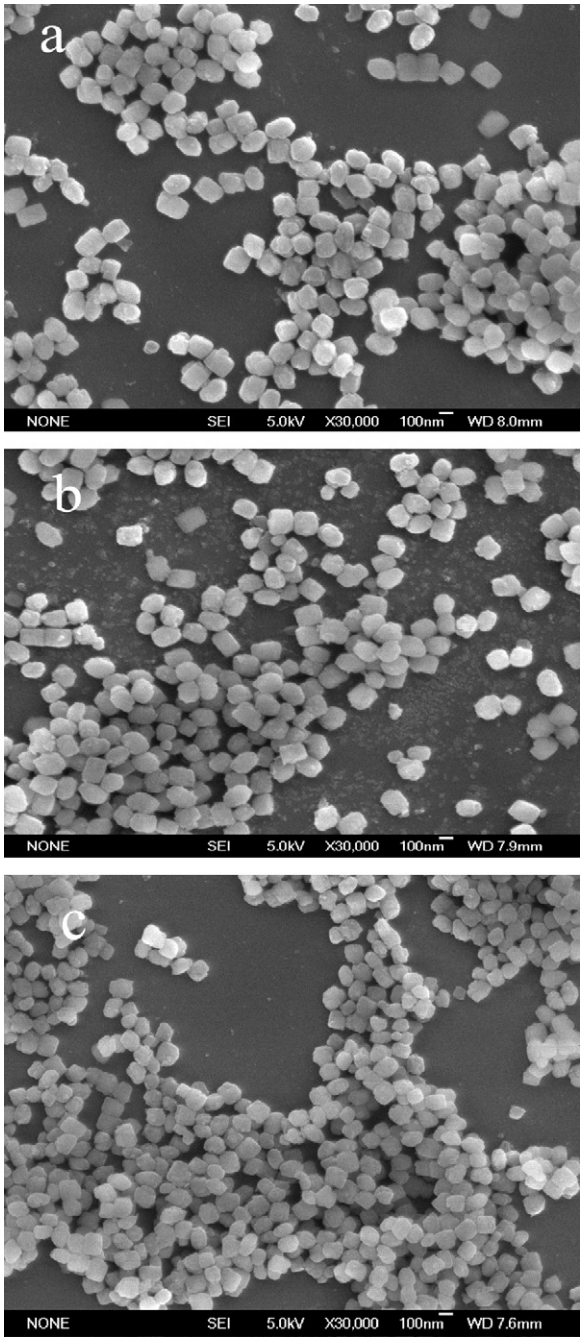

Fig. 3. SEM micrographs of the specimens (a) *A*, (b) *B* and (c) *C*.

the above assignment of the band at 270–280 nm is excluded. It was also reported that the band at 270–280 nm could be assigned to either partially polymerized hexa-coordinated Ti species containing Ti–O–Ti [23,24] or higher coordinated Ti species (in penta- or octa-hedral coordination) [25,26]. These Ti species are most possibly present in the framework of TS-1 rather than in a silicon-rich amorphous phase [27], due to the absence of amorphous phase as evidenced by the XRD and SEM results (see Figs. 1 and 3). In any case, the Ti species with a DR UV–vis band at 270–280 nm, which is present in all of the specimens *A*–*C*, is both inactive in the oxidation reaction and decomposition of H_2O_2 [21]. The most obvious difference identified by DR UV–vis spectra among the specimens *A*–*C* is that anatase is present in both the specimens *B* and *C*, with the content of anatase being higher for the specimen *B* than for the specimen *C*, but absent in the specimen *A*. Since no other phase

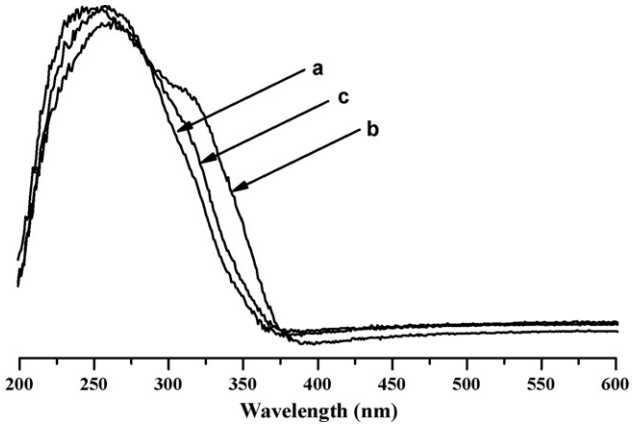

Fig. 4. DR UV–vis spectra of the specimens (a) *A*, (b) *B* and (c) *C*.

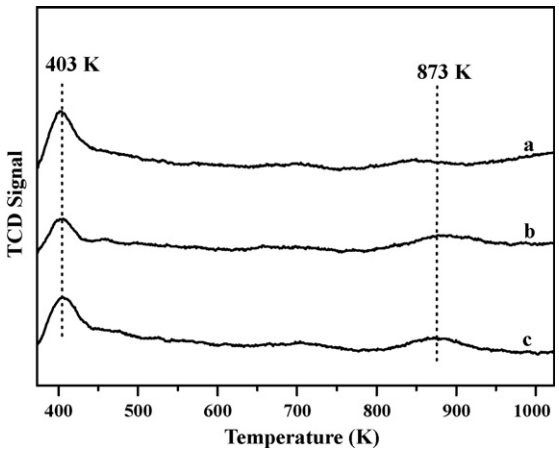

Fig. 6. NH_3-TPD profiles over the specimens (a) *A*, (b) *B* and (c) *C*.

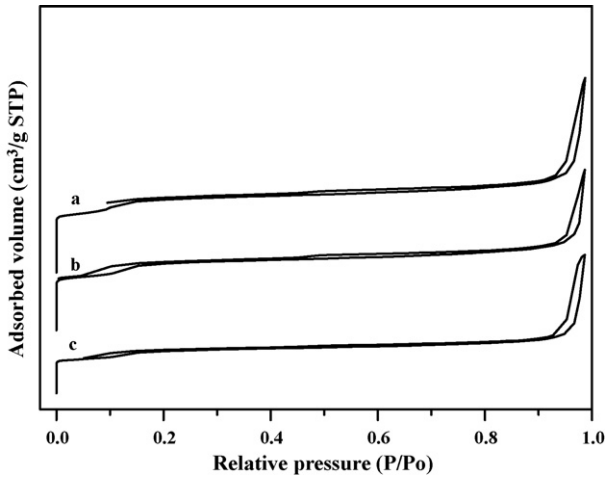

Fig. 5. N_2-physisorption at liquid nitrogen temperature over the specimens (a) *A*, (b) *B* and (c) *C*.

except TS-1 is detected by XRD (see Fig. 1), one can deduce that the anatase is highly dispersed in specimens *B* and *C*.

Fig. 5 shows the N_2 adsorption–desorption isotherms of the specimens *A*–*C*, which exhibit the typical characteristic of zeolite. In addition, these isotherms present also the hysteresis loops at the high values of relative pressure ($P/P_o > 0.9$), resulting from the large inter-crystal voids due to the aggregation of TS-1 crystals. The textural properties of the specimens *A*–*C* are listed in Table 2. One can see that the external surface area has an order specimen *A* < specimen *B* < specimen *C*, being due to the decrease of the average crystal size from the specimen *A* to *C*. The surface areas of the pores, the micropore volumes and the average micropore sizes for the specimens *B* and *C* are both smaller than those for the specimen *A*. It hints that the micropores of TS-1 are partially blocked for the specimens *B* and *C*, most possibly due to the high dispersion of anatase in the micropores of these two specimens. Since more amount of anatase is present in the specimen *B* than in the specimen *C*, as evidenced by DR UV–vis (see Fig. 4), both of the micropore volume and average micropore size for the specimen *B* are smaller than for the specimen *C*. The total pore volume and average pore size for the specimen *C* are larger than those for the specimen *A*. This is due that the average crystal size for the specimen *C* is smaller than for the specimen *A*, and thus, the specimen *C* is more easily congregated, presenting more inter-crystal voids. Because the average crystal size of the specimen *B* is situated between those of the specimens *A* and *C*, one can expect that the total pore volume and average pore size for the specimen *B* are also intervenient of those for the specimens *A* and *C*. The case is, however, opposite. This is most possibly due that the specimen *B* contains much larger amount of anatase than the specimen *C*. Besides the dispersion in the micropores of TS-1 for the specimen *B*, the anatase may also cover the surfaces of TS-1, reducing the inter-crystal voids.

Fig. 6 shows the NH_3-TPD profiles for the specimens *A*–*C*. One can see that a peak centered at ca. 403 K is present for all of the specimens. Besides, another peak centered at ca. 873 K is present both for the specimens *B* and *C*. Generally, in NH_3-TPD profiles, peaks are distributed into two regions, i.e., low-temperature (<673 K) and high-temperature (>673 K) regions, being attributed to the desorptions of NH_3 from weak and strong acid sites, respectively [28]. Many reports [29,30] have shown that TS-1 possesses only weak acid sites, which are due to the framework Ti. However, strong acid sites are also present in the TS-1 containing extra-framework Ti species [31]. Therefore, in our work, the peak centered at ca. 403 and 873 K originate, respectively, from the weak acid sites due to the framework Ti and the strong acid sites due to extra-framework Ti (anatase). The quantities of acid sites are calculated basing on the integral areas below the peaks and the results are listed in Table 3. It shows that the quantity of weak acid sites, i.e., the amount of framework Ti, follows the order specimen *A* ≈ specimen *C* > specimen *B*, being same as that identified by FT-IR. While strong acid sites, i.e., anatase, are absent in the specimen *A*, they are present in both of the specimens *B* and *C*, and the quantity of strong acid sites is larger for the specimen *B* than for the specimen *C*. This result is consistent with that obtained from the DR UV–vis.

Table 2
Textural properties of specimens *A*–*C*.

Specimens	S_{total} (m^2/g)	S_{ext} (m^2/g)	S_p (m^2/g)	V_p (cm^3/g)	$V_{m.p.}$ (cm^3/g)	D_p (Å)	$D_{m.p.}$ (Å)
A	376.8	52.55	324.2	0.47	0.154	49.66	6.51
B	358.4	59.94	298.5	0.39	0.142	43.79	5.99
C	361.3	71.39	289.9	0.55	0.145	63.33	6.31

Note: S_{total}, total surface area; S_{ext}, external surface area; S_p, total surface area of pores; V_p, total volume of pores; $V_{m.p.}$, total volume of micropores; D_p, average size of pores; $D_{m.p.}$, average size of micropores.

Table 3
Acidic properties of specimens *A*–*C*.

Specimens	Quantity of acid sites (mmol/g)	
	T_d = 403 K	T_d = 873 K
A	0.02392	0
B	0.01659	0.00953
C	0.02354	0.00817

Note: T_d refers to the temperature at the maximum of NH_3-TPD peak.

Table 4
Comparison of catalytic performances over specimens *A*–*C*.

Specimens	Conversion (%)	Selectivity (%)	Yield (%)
A	36.53	99.9	36.49
B	16.02	97.9	15.69
C	28.31	99.9	28.28

Temperature = 353 K; reaction duration = 2 h; catalyst/$C_6H_{12}O$ = 10 g/mol; $C_6H_{12}O$:NH_3:H_2O_2 = 1:1.5:1.2 (mole).

The above results of XRD, FT-IR, DR UV–vis, SEM, N_2-physisorption and NH_3-TPD indicate that the alkanol in the batch affects obviously the formation of TS-1. The presence of ethanol promotes the incorporation of Ti into the framework of TS-1 and retards the formation of anatase, however, the presence of IPA acts in the inverse direction.

The catalytic activity of the specimens *A*–*C* has been evaluated by the ammoximation of cyclohexanone with hydrogen peroxide and the result is listed in Table 4. One can see that both the conversion of cyclohexone and yield of cyclohexanone–oxime have the order specimen *A* > specimen *C* > specimen *B*. In the characterizations of FT-IR, DR UV–vis and NH_3-TPD, it has been identified that the content of framework Ti follows the order specimen *A* ≈ specimen *C* > specimen *B*; anatase is absent in the specimen *A*, but present in the specimen *B* and *C*, with its content being larger for the specimen *B* than for the specimen *C*. Thus, the larger content of framework Ti is responsible to the high catalytic performance of specimen *A*, whereas the presence of anatase results in the decomposition of H_2O_2 and in turn reduces the catalytic performances of specimens *B* and *C* [32]. In addition, the N_2-physisorption measurement has indicated that the microporosity has an order specimen *A* > specimen *C* > specimen *B*. The larger diffusion of specimen *A* contributes also to its higher catalytic performance than for specimens *B* and *C*.

4. Conclusion

TS-1 containing a relatively high content of framework Ti but without extra-framework Ti, anatase, has been successfully synthesized via the novel method developed in this paper. This method is characteristic of the replacement of IPA by ethanol and presence of ethanol all through the synthesis of TS-1, being in contrast to the method reported in the literature, in which IPA was employed during the hydrolysis of Ti source and was evaporated after the hydrolysis of Ti source. Compared to IPA, ethanol promotes the incorporation of Ti into the framework of TS-1 and also retards the formation of anatase. The TS-1 synthesized basing on ethanol exhibits a higher catalytic performance for ammoximation of cyclohexanone than that synthesized basing on IPA.

Acknowledgment

We are grateful to the financial supports from the Program for Lotus Scholar in Hunan Province, P.R. China.

References

[1] M. Taramasso, G. Perego, B. Notari, US Patent 4,410,501 (1983).
[2] B. Notari, Catal. Today 18 (1993) 163.
[3] P.T. Tanev, M. Chibwe, T.J. Pinnavala, Nature 368 (1994) 321.
[4] A.C.-K. Yip, F.L.-Y. Lam, X. Hu, Micropor. Mesopor. Mater. 120 (2009) 368.
[5] D.P. Serrano, R. Sanz, P. Pizarro, I. Moreno, P. de Frutos, S. Blázquez, Catal. Today 143 (2009) 151.
[6] R. Millini, E.P. Massara, G. Perego, G. Bellussi, J. Catal. (1992) 497.
[7] Y.G. Li, Y.M. Lee, J.F. Porter, J. Mater. Sci. 37 (2002) 1959.
[8] B. Notari, Stud. Surf. Sci. Catal. 37 (1988) 413.
[9] D.R.C. Huybrechts, P.L. Buskens, P.A. Jacobs, J. Mol. Catal. 71 (1992) 129.
[10] A. Thangaraj, R. Kumar, S.P. Mirajkar, P. Ratnasamy, J. Catal. 130 (1991) 1.
[11] A. Thangaraj, S. Sivasanker, J. Chem. Soc. Chem. Commun. (1992) 123.
[12] S.P. Mirajkar, A. Thangaraj, V.P. Shiralkar, J. Phys. Chem. 96 (1992) 3073.
[13] X.B. Ke, L. Xu, C.F. Zeng, L.X. Zhang, N.P. Xu, Micropor. Mesopor. Mater. 106 (2007) 68.
[14] J.L. Grieneisen, H. Kessler, E. Fach, A.M. Le Govic, Micropor. Mesopor. Mater. 37 (2000) 379.
[15] M.A. Uguina, D.P. Serrano, G. Ovejero, R.V. Grieken, M. Camacho, Appl. Catal. A 124 (1995) 391.
[16] X.S. Wang, X.W. Guo, Catal. Today 51 (1999) 177.
[17] M.A. Camblor, A. Corma, J. Pérez-Pariente, Zeolites 13 (1993) 82.
[18] J.S. Reddy, R. Kumar, J. Catal. 130 (1991) 440.
[19] G.Y. Zhang, J. Sterte, B.J. Schoeman, Chem. Mater. 9 (1997) 210.
[20] Z.H. Luan, L. Kevan, J. Phys. Chem. B 101 (1997) 2020.
[21] G. Li, X.S. Wang, X.W. Guo, S. Liu, Q. Zhao, X.H. Bao, L.W. Lin, Mater. Chem. Phys. 71 (2001) 195.
[22] F. Geobaldo, S. Bordiga, A. Zecchina, E. Giamello, Catal. Lett. 16 (1992) 109.
[23] M.R. Boccuti, K.M. Rao, A. Zecchina, G. Leofanti, G. Petrini, Stud. Surf. Sci. Catal. 98 (1989) 133.
[24] J.S. Choi, D.J. Kim, S.H. Chang, W.S. Ahn, Appl. Catal. A: Gen. 254 (2003) 225.
[25] K. Johannsen, A. Boisen, M. Brorson, I. Schmidt, C.J.H. Jacobsen, in: R. Aiello, G. Giordano, F. Testa (Eds.) Stud. Surf. Sci. Catal. 142 (2002) 109.
[26] D. Trong On, S.V. Nguyen, V. Hulea, E. Dumitriu, S. Kaliaguine, Micropor. Mesopor. Mater. 57 (2003) 169.
[27] N. Phonthammachai, M. Krissanasaeranee, E. Gulari, A.M. Jamieson, S. Wongkasemjit, Mater. Chem. Phys. 97 (2006) 458.
[28] M. Sawa, M. Niwa, Y. Murakami, Zeolites 10 (1990) 532;
H. Sato, Catal. Rev. Sci. Eng. 39 (1997) 395.
[29] R.S. Drago, S.C. Dias, J.M. McGilvray, A.L.M.L. Mateus, J. Phys. Chem. B 102 (1998) 1508.
[30] X.B. Ma, H.L. Guo, S.H. Wang, Y.L. Sun, Fuel Process. Technol. 83 (2003) 275.
[31] W.H. Liu, P. Guo, J. Su, J. Hu, Y.M. Wang, N. Liu, H.C. Guo, Chin. J. Catal. 30 (2009) 482.
[32] A.J.H.P. van der Pol, J.H.C. van Hooff, Appl. Catal. A: Gen. 92 (1992) 93.